Journal of the European Ceramic Society 17 (1996) 943–950
© 1997 Elsevier Science Limited
Printed in Great Britain. All rights reserved
0955-2219/97/$17.00
PII: S0955-2219(96)00162-8

Transport Properties of Titanium-Doped α-Alumina: Experimental Results

G. Petot-Ervas,[a] B. Saadi,[a] C. Petot[a] & M. Loudjani[b]

[a]CNRS-URA 453, Laboratoire de Chimie Physique du Solide, Ecole Centrale de Paris, 92295 Chatenay Malabry, France
[b]ISMA-Laboratoire de Métallurgie Structurale, Université Paris XI, Bât. 413, 91405 Orsay, France

(Received 6 March 1996; revised version received 26 July 1996; accepted 5 August 1996)

Abstract

Electrical conductivity, ionic transference number and chemical diffusion values of titanium-doped α-alumina single crystals were measured at high temperature as a function of orientation, oxygen partial pressure and temperature. This set of results is consistent with a model in which aluminum vacancies (three times ionized) are the prevailing defects. A small anisotropic effect was observed on the electrical conductivity values. This effect is more pronounced on the chemical diffusion values, obtained in air. A decrease of the chemical diffusion was observed between 1350 and 1450°C for the sample cut parallel to the c axis and between 1400 and 1530°C for the sample cut perpendicular to the c axis. This unexpected variation has been attributed to short circuit effects caused by the formation of TiO_2 *precipitates in preferred planes. The solubility limit of titanium in alumina deduced from these results is close to 0·05% in wt at 1530°C. Also, the electrical conductivity measurements performed under* CO/CO_2 *mixtures have allowed us to show the effect of carbon on the transport properties of alumina. This effect has been only detected when titanium forms* TiO_2 *precipitates in alumina. XPS analysis shows the presence of carbon bound to titanium and suggests, in agreement with phase diagram calculations, that carbon reacts with* TiO_2 *to form oxy-carbide precipitates. © 1997 Elsevier Science Limited.*

1 Introduction

Due to its narrow range of departure from stoichiometry the defect chemistry in α-alumina is still uncertain. Both Frenkel and Schottky defects have been proposed in the literature.[1-3] Experimental results with doped materials should allow, in principle, to identify the defect model. Indeed, a Frenkel disorder of aluminum leads to aluminum vacancies by donor doping or aluminum interstitials by acceptor doping, while a Frenkel disorder of oxygen would lead to oxygen interstitials or oxygen vacancies by donor or acceptor doping, respectively. If Schottky disorder is dominant doping with a donor produces alumina vacancies and doping with an acceptor causes oxygen vacancies to form. In the presence of dopant, the major disorder mechanism can be obtained generally by a study of the oxygen pressure dependence of the transport properties such as the electrical conductivity or the self diffusion, for example. Each defect model used to interpret the results has characteristic parameters which can be calculated from such studies and compared with the theoretical values.[1] This comparison allows in principle to identify the prevailing defects. Nevertheless, one of the most difficult problems in interpreting alumina data is the influence of unavoidable accidental impurities which are present even in the highest purity crystals. Indeed, the values of the characteristic parameters are in many cases too close[1,4] and the presence of impurities should be taken into account in the interpretation of the data if the amount of dopant is not large enough compared with the impurity level which is generally higher than 50 ppm.

The main impurities found in alumina are calcium, magnesium, iron and silicon. They can be present in the starting powder or introduced during the technological process of preparing the samples. If the amount of doping elements is not sufficiently large these impurities, which can act as acceptor (Ca, Mg, Fe) or donor (Fe, Si) in alumina, can control the transport properties and generally more than one solute cation should be taken into account in the interpretation of the data. This means that samples from different batches represent more often different materials. Consequently, the reliability of defect models cannot be checked satisfactorily from the results obtained by different authors, mainly when little is known about the purity of the materials used. Only the data obtained from different experimental approaches on samples from the same batch can allow identification with a higher degree of certainty of the defects responsible for the matter transport in a given alumina. Consequently, despite the numerous investigations of alumina over the years, further experimental and theoretical studies are required to clarify the nature of the point defects responsible for atomic transport. Alumina being an important ceramic for high-temperature applications, such studies will allow an understanding of the dependence on composition, oxygen partial pressure, microstructure and temperature of its physical properties such as creep, electrical conductivity, diffusion or sintering.

Optical absorption, electrical conductivity and transference numbers have been measured by Kröger *et al.*[5] on alumina single crystals doped with 430 ppm titanium. These authors have observed that the electrical conductivity is isotropic. It is ionic at high and electronic at low P_{O_2}. Their results have been accounted for on the basis of a defect model dominated by aluminum vacancies three times ionized (V'''_{Al}). Furthermore, the analysis of the electrical conductivity measurements obtained at equilibrium and under conditions where equilibrium with the surrounding atmosphere is not reached have allowed them to calculate the position of the energy level of titanium (Ti^{x}_{Al}) in the forbidden gap and the temperature dependence of the mobility of the aluminum vacancies. The chemical diffusion coefficient has been measured by Jones *et al.*[6] (for single crystals doped with 500 ppm Ti) and by Kröger *et al.*[7] (for polycrystalline samples doped with 7000 ppm Ti) using the change of colour of α-alumina doped with titanium, which is pink when it is annealed in a reducing atmosphere and not coloured when Ti^{3+} is oxidized to Ti^{4+}. The values of the chemical diffusion coefficient have been determined from the kinetics of movement of the colour front for partially oxidized or reduced samples. On the other hand, the optical absorption responsible for the pink colour of the reduced samples has allowed Kröger and co-workers[5,7] to determine the concentration ratio of Ti^{3+} and Ti^{4+} as a function of P_{O_2} on quenched samples previously annealed under different oxygen partial pressures.

Defect calculations in α-alumina have been performed by Catlow *et al.*[2] and more recently by Grimes[3] using a computer simulation method. A more extensive set of defects has been considered by Grimes, but their results show a quite good agreement when it is possible to make comparison. They are then a valuable support for the analysis of the experimental data. In a general way, they suggest the dominance of a Schottky disorder and a significant lowering of impurity solution energies by defect clustering. In the case of Ti-doped alumina, they predict that the solution of TiO_2 takes place via the formation of substitutional defects ($Ti^{\bullet}_{Al}$) electrically compensated by the creation of cation vacancy (V'''_{Al}). They also found that the preference for this solution mechanism becomes much stronger when titanium/vacancy clusters ($n \times Ti^{\bullet}_{Al}\ V'''_{Al}$) are considered. This conclusion is supported by the experimental results reported recently by Moon and Philips.[8] In addition, Grimes predicts also that the cosolution of magnesia and titania is more favourable than for either oxide separately, due to a lowering of the cosolution energy. The defects formed by the tetra- and divalent ions in substitution position (Mg'_{Al} and $Ti^{\bullet}_{Al}$) compensate for each other and the creation of vacant sites is not necessary. The presence of one oxide then increases significantly the solution limit of the other. Conversely, whereas the presence of titanium assists the solution of CaO, he found that CaO does not increase the solution limit of TiO_2 due to a calcium ion size effect.

The present work studies the influence of titanium on the transport properties of alumina. The experimental data are for electrical conductivity, chemical diffusion and XPS analysis. They have been obtained with single crystals doped with 500 ppm in weight of titanium (3×10^{19} atom per cm^3 or 11×10^{-4} atom per Al_2O_3 mole) and with undoped titanium polycrystals. The different samples have been obtained from the same starting powder. In such conditions the nature and the amount of impurities is approximately the same in the different materials. This study makes it possible to illustrate the effect of titanium on the transport properties of alumina.

2 Experimental Procedure

The doped samples were cut from a single crystal grown by the Verneuil technique from high purity alumina powder. The undoped polycrystalline samples were prepared by hot pressing the powder in a graphite die for 0·25 h at 1550°C under a pressure of 30 MPa. One can point out that we have observed previously[9] that the microstructure does not affect the transport properties of alumina at high temperature ($T > 1500$°C) . Table 1 gives the impurity concentrations found in the pure and doped materials. The samples were machined with

Table 1. Impurities in alumina found by spectrochemical analysis (ppm in wt)

B < 5	Cu < 1	Mn < 1	Ni < 3
Ca < 3	Co < 3	Mo < 3	Si < 5
Fe < 5	Ga < 3	Na < 25	
Cr < 1	Mg < 1	Pb < 1	Zn < 50

a diamond saw in order to obtain discs of approximately 1 to 1·2 mm thickness and 9 mm diameter for the electrical conductivity measurements. Samples for emf measurements were cut to a thickness of approximately 0·7 mm in order to reduce the electrical resistance while retaining the mechanical resistance of the material. The electrical conductivity measurements were performed with alternating current (1592 Hz) by a three-contact method using a Wayne Kerr bridge.[9,10] This method with a volume guard eliminates the surface and gas-phase conduction. Electrical connections were made with platinum wires and foils. The equilibrium atmospheres were established with oxygen/air, air/argon and CO/CO_2 mixtures. Oxygen partial pressures were measured by means of a zirconia electrochemical gauge placed in the laboratory tube so that the temperature at the electrode level was ≤ 1400°C, to prevent the electrolyte and the electrical junctions from ageing. The electrical conductivity was measured either after the samples were equilibrated at various T and P_{O_2} or during the equilibration of the gas-oxide system. The ionic transference number was obtained from emf measurements of electrochemical cells[11] which can be schematized as follows:

$$\text{Pt}, (P_{O_2})_1/\text{Al}_2\text{O}_3/\text{Pt}, (P_{O_2})_2 \qquad (1)$$

with Pt contact leads and where $(P_{O_2})_1 = 0{\cdot}21$ atm and $(P_{O_2})_2$ is variable (≤ 1 atm).

The sealing between the two electrode compartments was achieved by two platinum rings and alumina tubes placed on opposite surfaces of the alumina disc. The emf (E) of such cells is given by:[1,11]

$$E = (RT/4F) \int_{0\cdot 21}^{(P_{O_2})_2} t_i d \ln P_{O_2} \qquad (2)$$

where R is the gas constant, T (in K) the temperature, F the Faraday constant, $t_i = \sigma_i/\sigma$ the ionic transference number, σ_i the ionic conductivity and σ the total conductivity. Differentiation of this expression for $(P_{O_2})_2$ keeping $(P_{O_2})_1$ constant gives t_i at $(P_{O_2})_2$:

$$t_i = (\delta(4EF/RT)/\ \delta \ln (P_{O_2})_2)\ (P_{O_2})_1 \qquad (3)$$

t_i is obtained from the slope of the plot of $4EF/RT$ versus $\ln (P_{O_2})_2$.

3 Experimental Results

3.1 Electrical conductivity measurements at thermodynamic equilibrium

The electrical conductivity measurements performed with the doped samples cut perpendicular and parallel to the c axis are shown in Figs 1 and 2. These results can be expressed by the following relation:[9,11]

$$\sigma = B \exp -\Delta H_\sigma/RT\ (P_{O_2})^\alpha \qquad (4)$$

where α characterises the prevailing charged defects (as seen later) and ΔH_σ is the enthalpy of conductivity.

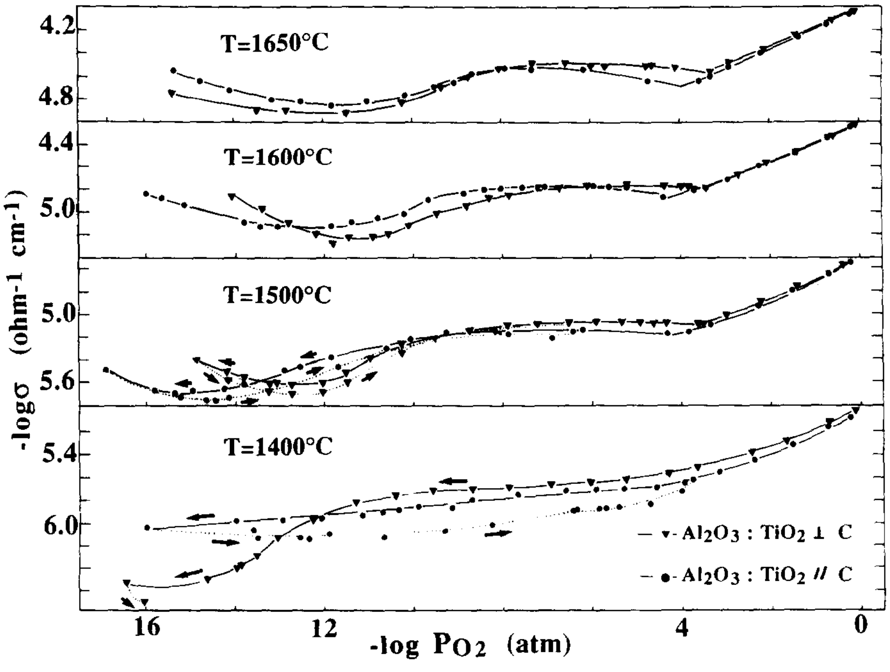

Fig. 1. Oxygen partial pressure dependence of the electrical conductivity of titanium-doped α-alumina single crystals cut perpendicular and parallel to the c axis.

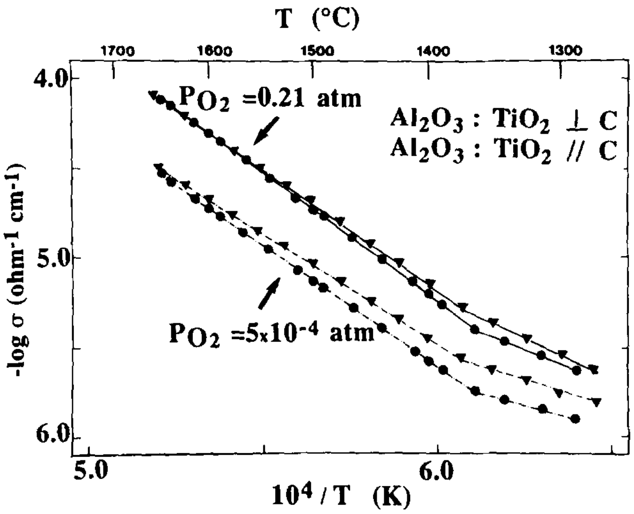

Fig. 2. Temperature dependence of the electrical conductivity of titanium-doped single crystals of α-alumina cut perpendicular and parallel to the c axis.

3.1.1 Electrical conductivity results for oxygen partial pressures higher than 10^{-5} atm

In this oxygen partial pressure range a small anisotropy was observed (Fig. 1). Whatever the temperature, with increasing P_{O_2} the electrical conductivity increases slowly up to 1 atm and the variation log σ versus log P_{O_2} is nearly linear. In Table 2 we report the values obtained for the parameter α defined as follows:

$$\alpha = (\delta \ln \sigma / \delta \ln P_{O_2})_T \tag{5}$$

The values increase slowly with temperature and they are close to the theoretical value of 3/16 at 1650°C which corresponds to aluminum vacancies three times ionized as suggested previously[2,3,5] in titanium-doped α-alumina. The results obtained with the undoped sample (plotted in Fig. 3) show that the presence of titanium increases the electrical conductivity of the material in this oxygen partial pressure range. The temperature dependence of the electrical conductivity in air or under an oxygen partial pressure equal to 5×10^{-4} atm is plotted in Fig. 2 and the analytical equations are given in Table 3. A break is observed at about 1350–1380°C. As we shall see later (cf. Section 3.2) this break corresponds probably to the limit of solubility of titanium in α-alumina. The results obtained at low temperature correspond then to samples in which the excess dopant is precipitated.

Table 2. Values of the parameter α determined for P_{O_2} higher than 10^{-5} atm

T(°C)	α
1650	0·176
1600	0·171
1500	0·169
1400	0·168

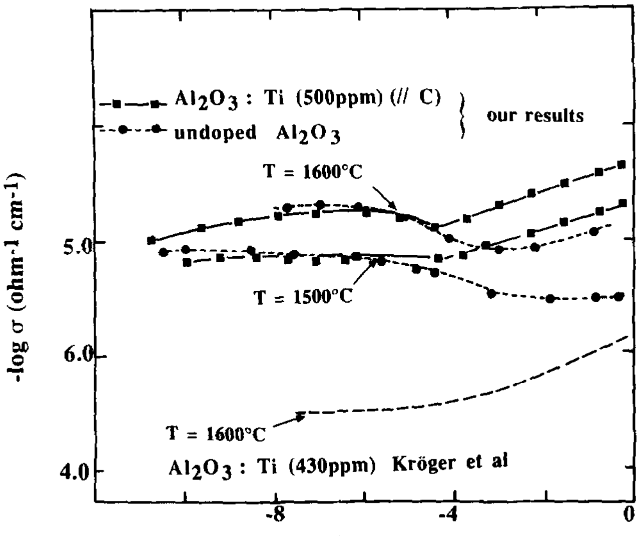

Fig. 3. Oxygen partial pressure dependence of the electrical conductivity of an undoped polycrystalline sample and of a titanium-doped alumina single crystal prepared from the same starting powder. Comparison with the experimental results obtained by Kröger *et al.*[5] with a single crystal doped with 430 ppm Ti.

The concentration of point defects in this temperature range is then determined by the saturation solubility of titanium in alumina. One can point out that the variations of conductivity with T or P_{O_2} in this oxygen partial pressure range are closely related to those observed by Mohapatra and Kröger[5] while the values of σ are higher than those measured by these authors (Fig. 3).

3.1.2 Electrical conductivity for oxygen partial pressures lower than 10^{-5} atm

In this oxygen partial pressure range the measurements have been performed under argon or CO/CO_2 mixtures. With decreasing P_{O_2}, there is almost no oxygen pressure dependence of the electrical conductivity values obtained with the titanium-doped samples until nearly 10^{-8} atm. As shown in Fig. 3 this behaviour is similar to that observed by Mohapatra and Kröger[5] whose measurements have been performed in the oxygen partial pressure range 10^{-8}–1 atm. Then, for $P_{O_2} < 10^{-8}$ atm, (Fig. 1) the values of conductivity decrease slowly, reach a shallow minimum and increase slightly. A small anisotropic effect has been observed in the low oxygen partial pressure range and a hysteresis phenomenon has been detected for temperatures $\leq$ 1500°C (Fig 1). Indeed, the electrical conductivity values measured with increasing P_{O_2} are lower than those obtained with decreasing the oxygen partial pressure. For $P_{O_2} < 10^{-5}$ atm, the measurements have been performed under CO/CO_2 mixtures and we have observed that the hysteresis phenomenon increases with increasing amount of CO in the gaseous phase in equilibrium with the

Table 3. Temperature dependence of the electrical conductivity in air and under an oxygen partial pressure of 5×10^{-4} atm (the activation energy of conductivity is in eV)

T	P_{O_2} *(atm)*	*Parallel to c axis* $(\Omega^{-1}\ cm^{-1})$	*Perpendicular to c axis* $(\Omega^{-1}\ cm^{-1})$
> 1350°C	0·21	$(20 \pm 0{\cdot}14)10^2 \exp(-\frac{2{\cdot}83 \pm 0{\cdot}03}{kT})$	$(9 \pm 0{\cdot}14)10^2 \exp(-\frac{2{\cdot}70 \pm 0{\cdot}03}{kT})$
	$5{\cdot}10^{-4}$	$(3{\cdot}06 \pm 0{\cdot}006)10^2 \exp(-\frac{2{\cdot}68 \pm 0{\cdot}02}{kT})$	$(0{\cdot}75 \pm 0{\cdot}006)10^2 \exp(-\frac{2{\cdot}44 \pm 0{\cdot}02}{kT})$
< 1350°C	0·21	$(0{\cdot}17 \pm 0{\cdot}002) \exp(-\frac{1{\cdot}51 \pm 0{\cdot}07}{kT})$	$(1{\cdot}45 \pm 0{\cdot}002) \exp(-\frac{1{\cdot}78 \pm 0{\cdot}07}{kT})$
	$5{\cdot}10^{-4}$	$(2{\cdot}30 \pm 0{\cdot}02)10^{-3} \exp(-\frac{1{\cdot}01 \pm 0{\cdot}07}{kT})$	$(10{\cdot}0 \pm 0{\cdot}02)10^{-3} \exp(-\frac{1{\cdot}19 \pm 0{\cdot}07}{kT})$

sample. It decreases when the temperature increases and it disappears at T>1500°C. It may be pointed out that a similar effect has not been detected in the undoped titanium sample prepared from the same alumina powder (Fig. 3). Furthermore, it was not found in earlier studies performed with yttrium- or chromium-doped alumina samples[9,12] but was observed in a polycrystalline sample whose transport properties are controlled by silicon.[13] As we shall see later, this effect seems to be due to the formation of carbide or oxy-carbide precipitates (cf. Section 3.3).

For oxygen partial pressures between 10^{-5} and 10^{-12} atm (Fig. 3) the electrical conductivity values measured with the doped and the undoped samples are relatively close. This means that the impurities present in the crystals control, almost in part, the transport properties of the samples, due to the decreasing concentration of Ti^{4+} when the oxygen activity decreases.[5]

3.1.3 Emf measurements

The results obtained are reported in Table 4. In agreement with Mohapatra and Kröger[5] we have observed that the ionic conductivity prevails at high oxygen partial pressures while it is electronic at low P_{O_2}.

3.2 Electrical conductivity measurements during equilibration of the gas-oxide system — chemical diffusion

Chemical diffusion coefficient values were evaluated from the electrical conductivity measurements performed during the re-equilibration of the oxide after a sudden change in the oxygen partial pressure, at constant temperature. Taking into account the geometry of the sample, the electrical conductivity $\sigma(T)$ during the equilibration of the crystal is related to the chemical diffusion coefficient ($\tilde{D}$) by the relation:[14]

$$(\sigma_t - \sigma_\infty)/(\sigma_0 - \sigma_\infty) = (8/\pi^2)\exp(\pi^2 \tilde{D} t/h^2) \quad (6)$$

where h is the thickness of the sample, σ_0 the conductivity at time zero, when P_{O_2} is changed, and σ_∞ the conductivity when the new equilibrium is reached.

The results obtained with samples cut perpendicular and parallel to the c axis are plotted in Fig. 4. This figure shows that the chemical diffusion is anisotropic. A break is observed in the Arrhenius curve at about 1350°C for the sample cut parallel to the c axis and at about 1400°C for the sample cut perpendicular to the axis. Above these temperatures the chemical diffusion coefficient values decrease while the temperature increases, but the values increase again from about 1450°C for the sample cut parallel to the c axis and 1530°C for that cut in the perpendicular direction. The analytical equations of the results obtained in the high and low temperature ranges are reported in Table 5.

The comparison of our results with those published in the literature[6,7] (Fig. 4) shows that a good agreement is observed at high temperature between the results we have obtained with the sample cut perpendicular to the c axis and those

Table 4. Ionic transference number in Ti-doped α-alumina

Range of P_{O_2} / *Temperature (°C)*	*0·4 atm to 0·2 atm*				*0·2 atm to* 5×10^{-4} *atm*			
	1400	1500	1600	1650	1400	1500	1600	1650
t_i	0·74	0·89	0·80	0·97	0·05	0·04	0·04	0·10

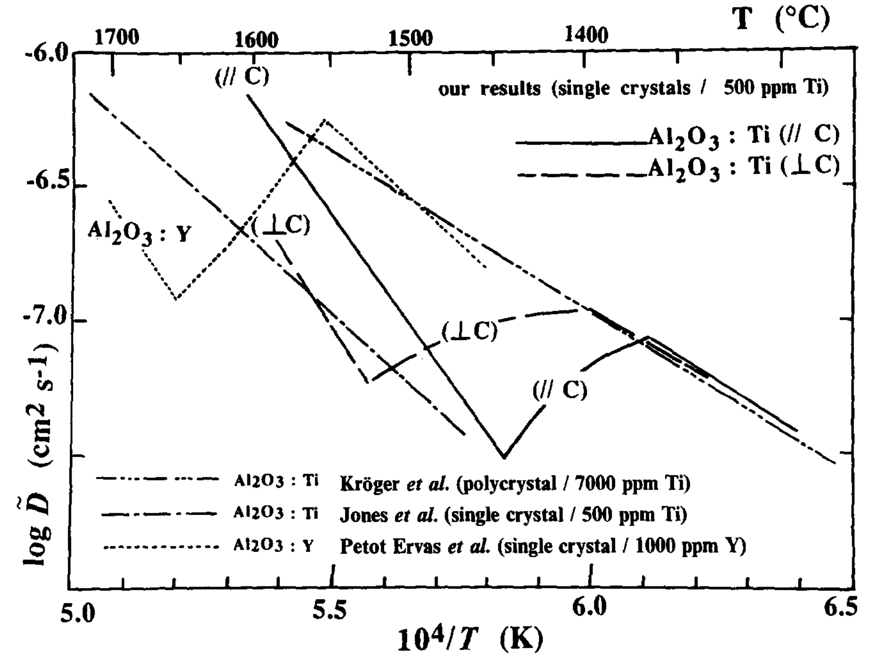

Fig. 4. Chemical diffusion values in air. Comparison with literature results, Refs 4–6.

determined by Jones *et al.*[6] for a single crystal doped with 500 ppm Ti. In the low temperature range (T< 1400°C) our results are in good agreement with those obtained by Wang and Kröger[7] for polycrystalline samples doped with 7000 ppm Ti and in which the excess dopant has precipitated at grain boundaries.[7] This agreement suggests that the results we have obtained for temperatures lower than 1400°C correspond to samples in which the concentration of point defects and electronic carriers is determined by the saturation solubility of titanium in Al_2O_3. The solubility of titanium found by Wang and Kröger[7] close to 6 × 10^{-4} atoms/molecule at 1520°C (the amount of titanium in our samples is 11 × 10^{-4} atoms/molecule) confirms this analysis as well as the observations of Philips *et al.*[15] on quenched samples. One can recall that these last authors have identified long needle-shaped precipitates in titanium-doped (500 and 800 ppm) α-alumina previously annealed in air at 1400°C. These needles have been previously observed by Pletka *et al.*[16] who accepted the view that these precipitates must be some metastable phase more aluminum-rich than Al_2TiO_3, the expected equilibrium phase. However, in their work Philips *et al.*[15] have identified, by both electron diffraction and microchemical analysis, the needles as TiO_2 precipitates. The length of these particles ranges up to some hundred microns while the width is close to 0·5 microns and the height usually smaller than the width.[15] These rutile needles lies in the basal plane and their axis is parallel to the three <1010> directions of alumina. By optical microscopical observations be performed on samples cut parallel to the c axis (perpendicular to the needles) we have also observed that these needles appear in preferential planes[10,15] which can extend over several hundred microns through the sample. These preferential planes may be subgrain boundaries as suggested previously by Pletka *et al.*[16]

It may be noted that the short-circuit effects are observed until 1530°C for samples cut perpendicular to the c axis while they are observed only until 1450°C for samples cut in the other direction. This unexpected behaviour may be ascribed to the distribution of the needles in preferential planes which can extend over several hundred microns through the thickness of the samples cut perpendicular to the c axis. This non-random distribution of the needles makes their contribution non-negligible until all the TiO_2 precipitates are

Table 5. Temperature dependence of the chemical diffusion in the high and low temperature ranges (activation energy of diffusion in eV)

T	*< 1350°C*	*>1450°C*
$\tilde{D}$ (parallel to c axis) (cm^2 s^{-1})	$(4{\cdot}66 \pm 0{\cdot}22)10^6 \exp -\frac{4{\cdot}82 \pm 0{\cdot}50}{kT}$	$(5{\cdot}92 \pm 0{\cdot}12) \exp -\frac{2{\cdot}55 \pm 0{\cdot}85}{kT}$
$\tilde{D}$ (perpendicular to c axis) (cm^2 s^{-1})	$(1{\cdot}22 \pm 0{\cdot}29)10^4 \exp -\frac{4{\cdot}00 \pm 0{\cdot}85}{kT}$	$(2{\cdot}74 \pm 0{\cdot}14) \exp -\frac{2{\cdot}44 \pm 0{\cdot}85}{kT}$

practically dissolved in the samples cut perpendicular to the c axis. This suggests that the limit of solubility of Ti in α-alumina is close to 500 ppm at 1530°C, in agreement with the value proposed by Mohapatra and Kröger.[5] One can point out that the breaks observed at about 1350–1400°C, both on the graphs of log $\tilde{D}$ and log σ as a function of $1/T$, have probably the same origin, i.e. the solubility limit of titanium in alumina. One can recall that breaks have also been observed on the temperature dependence of the electrical conductivity and chemical diffusion values (Fig. 4) of yttrium-doped alumina samples,[9] but in different temperature ranges. The breaks have then been attributed to short-circuit effects caused by yttrogarnet precipitates and have allowed us to estimate the limit of solubility of yttrium in alumina as close to 1000 ppm at 1550°C.

3.3 X-ray photoelectron spectroscopy (XPS) — analysis of samples annealed under oxygen or CO/CO_2 mixtures

XPS analysis[13] has allowed us to detect on samples treated at 1400°C for one week under CO/CO_2 mixtures ($P_{O_2} = 10^{-17}$ atm) a peak at 281 eV (Fig. 5) which corresponds to the binding energy of carbon–titanium. Analysis has been performed after the surface layers of the samples have been removed by argon sputtering. The intensity of this peak is not constant through the sample (Fig. 5) and the peak at 281 eV disappears when the sample is treated with oxygen. These results suggest the formation of localized titanium carbide or oxy-carbide precipitates in titanium-doped alumina samples annealed under CO/CO_2 mixtures.

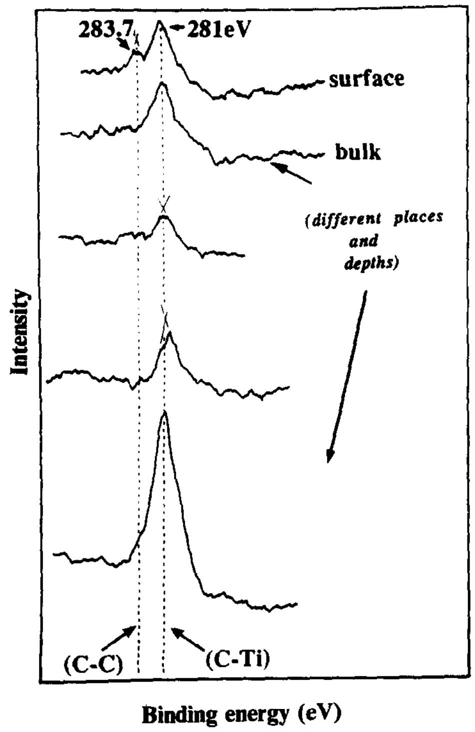

Fig. 5. X-ray photoelectron spectrum of alumina doped with titanium (excited by Mg-$K\alpha$ recorded with a constant analyser energy of 100 eV).

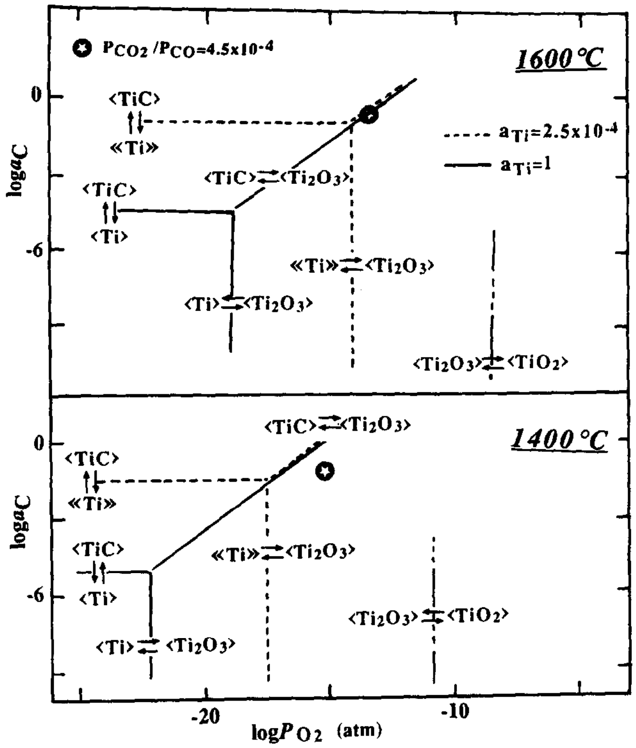

Fig. 6. Stability range at 1600°C of titanium (a_{Ti} = 1) and titanium compounds ($a_{Ti} = 2{\cdot}5 \times 10^{-4}$) as a function of the carbon and oxygen activity ($a_O = P_{O_2}^{1/2}$).

As mentioned previously, the effect of CO/CO_2 mixtures on the electrical conductivity measurements (hysteresis phenomenon) appears for temperatures ≤1500°C, i.e. for temperatures at which TiO_2 precipitates are found in the samples. This set of results suggests that carbon dissolves from the gas phase in alumina, as proposed by different authors in the literature.[17–21] In the presence of TiO_2 particles, carbon reacts to form titanium carbide or oxy-carbide precipitates. The presence of this new phase changes the local chemical equilibrium and consequently the concentration of defects responsible for the transport properties. This assumption is confirmed by the range of stability of titanium and titanium compounds (Fig. 6) determined from the thermodynamical equilibrium data.[22] The results reported in Fig. 6 show that TiC starts to precipitate at 1600°C in titanium solid solutions ($a_{Ti} = 2{\cdot}5 \times 10^{-4}$) when the oxygen partial pressures in the surrounding atmosphere is close to 10^{-13} atm and the carbon activity to 10^{-1}.

4 Conclusion

In this study measurements of electrical conductivity and ionic transport number indicate that titanium-doped α-alumina is an ionic conductor at high P_{O_2} and an electronic conductor at low P_{O_2}.

In the high oxygen partial pressure range the results are consistent with the presence of aluminum vacancies three times ionized suggested previously from theoretical and experimental works. Nevertheless, for oxygen partial pressures lower than 10–4 atm our results suggest that the impurities present in the undoped and doped material partially control the transport properties of the titanium-doped single crystals due to the decrease of the concentration of Ti^{4+}. Chemical diffusion data have been deduced from electrical conductivity measurements performed during the equilibration of the gas-oxide system. We have observed that the chemical diffusion is anisotropic. An increase of $\tilde{D}$ has been observed when the temperature decreases between 1520 and 1350°C, according to the crystallographic orientation. This unexpected variation was attributed to short circuit effects caused by the precipitation of TiO_2. This assumption was confirmed by the temperature dependence of the electrical conductivity and has allowed us to suggest for the limit of solubility of Ti in alumina a value close to 500 ppm in wt at 1530°C. Furthermore, the electrical conductivity results obtained with the doped samples have allowed us to show the effect of CO/CO_2 mixtures on the transport properties of α-alumina. This effect has been observed only when titanium forms TiO_2 precipitates in alumina. Consequently, it has been proposed, in agreement with XPS results and phase diagram calculations, that carbon reacts with TiO_2 to form oxy-carbide precipitates. This new phase changes the local chemical equilibrium in the sample and consequently the concentration of defects responsible for the transport properties.

Acknowledgement

The authors thank C. Severac (LMS Orsay) for his collaboration.

References

1. Kröger, F. A., Defect related properties in α-alumina. *Solid State Ionics*, 1984, **12**, 189–199.
2. Catlow, C. R. A., James, R., Mackrodt, W. C., and Stewart, R. F., Defect energies in α-Al_2O_3 and rutile TiO_2. *Physical Review*, 1982, **25**, 1006–1026.
3. Grimes, R. W., Solution of MgO, CaO, and TiO_2 in α-Al_2O_3. Science of alumina. *J. Am. Cer. Soc.*, 1994, **77**(2), 378–384.
4. El-Aiat, M. M., and Kröger, F. A., Determination of the parameters of native disorder in α-alumina. *J. Am. Cer. Soc.*, 1982, **65**, 162–166.
5. Mohapatra, S. K. and Kröger, F. A., Defect structure of α-alumina doped with titanium. *J. Am. Cer. Soc.*, 1977, **60**, 381–387.
6. Jones, T. P., Coble, R. L. and Mogab, C. J., Defect diffusion in single crystals of alumina. *J. Am. Cer. Soc.*, 1969, **52**, 331–334.
7. Wang, H. A. and Kröger, F. A., Chemical diffusion in polycrystalline alumina. *J. Am. Cer. Soc.*, 1980, **63**, 613–619.
8. Moon, A. R. and Philips, M. R., Defect clustering in H, Ti: α-Al_2O_3. *J. Phys. Chem. Solids*, 1991, **52**, 1987–1999.
9. Petot-Ervas, G., Deweirder, D., Loudjani, M., Lesage, B. and Huntz, A. M., The influence of the microstructure on the transport properties of yttrium-doped alumina. *Adv. in Cer.*, 1987, **23**, 125–135.
10. Saadi, B., Transport properties of Ti-doped α-Al_2O_3. Thesis, University Paris XIII, 1986.
11. Kofstad, P., *Non-stoichiometry, Diffusion and Electrical Properties in Binary Metal Oxides.* Wiley-Interscience, New York, 1972.
12. Lesage, B., Huntz, A. M., Ochin, P., Saadi, B. and Petot-Ervas, G., Influence of chromium and yttrium on the transport phenomena in monocrystalline alumina. *Solid State Ionics*, 1984, **12**, 243–251.
13. Petot-Ervas, G., Petot, C., Lesage, B., Huntz, A. M. and Severac, C., Localization of carbon and its influence on the transport properties of oxides. *Solid State Ionics*, 1988, **28–30**, 1244–1249.
14. Petot-Ervas, G., Radji, O. and Sossa, B., Chemical diffusion measurements in pure and Li-doped cobaltous oxide. *Radiation Effects*, 1983, **75**, 301–308.
15. Philips, D. S., Heuer, A. H. and Mitchell, T. E., Precipitation in star sapphire. *Phil. Mag.*, 1985, **12**, 385–404, 405–416.
16. Pletka, B. J., Mitchell, T. E. and Heuer, A. H., Mechanical behavior of materials. Kyoto: Society of Materials Science., 1972, 413–422.
17. Kofstad, P., Diffusional transport in MnO. *Solid State Ionics*, 1984, **12**, 101–111.
18. Freund, F., Debras, G. and Demortier, G., *J. Am. Cer. Soc.*, 1973, **61**, 429.
19. Kathrein, H. and Freud, F., *J. Phys. Chem. of Solids*, 1983, **44**, 177.
20. Routbort, J. L., Goretta, K. C. and Castaing, J., *Mater. Letters*, 1986, **4**, 149.
21. Jimenez, M., Castaing, J., Rodriguez, A. and Marquez, R., *J. Phys. Chem. of Solids*, 1986, **47**, 331.
22. Kubachewski, O. and Alcock, C. B., *Metallurgical Thermo-chemistry*, 5th edn, *International Series on Materials Science and Technology*, Pergamon Press, Oxford, vol. 24, 1979.